SINTEF
PROCEEDINGS
2

Proceedings of the 12th International Conference on Computational Fluid Dynamics in the Oil & Gas, Metallurgical and Process Industries

Progress in Applied CFD – CFD2017

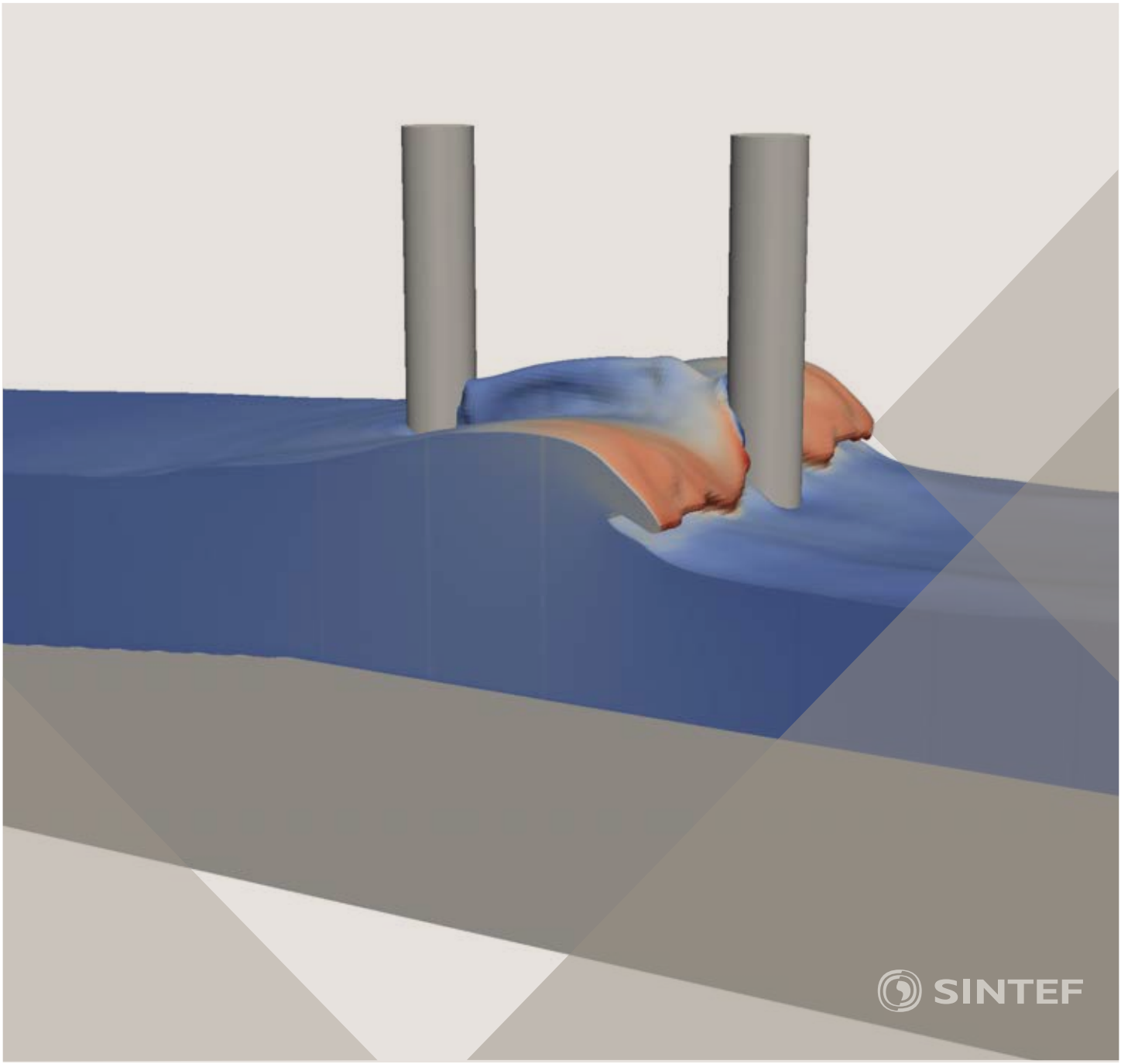

SINTEF Proceedings

Editors:
Jan Erik Olsen and Stein Tore Johansen

Progress in Applied CFD – CFD2017

Proceedings of the 12th International Conference on Computational Fluid Dynamics in the Oil & Gas, Metallurgical and Process Industries

SINTEF Academic Press

SINTEF Proceedings no 2
Editors: Jan Erik Olsen and Stein Tore Johansen
Progress in Applied CFD – CFD2017
Selected papers from 10th International Conference on Computational Fluid Dynamics in the Oil & Gas, Metallurgical and Process Industries

Key words:
CFD, Flow, Modelling

Cover, illustration: Arun Kamath

ISSN 2387-4295 (online)
ISBN 978-82-536-1544-8 (pdf)

SINTEF Academic Press
Address: Forskningsveien 3 B
PO Box 124 Blindern
N-0314 OSLO
Tel: +47 73 59 30 00
Fax: +47 22 96 55 08

www.sintef.no/byggforsk
www.sintefbok.no

SINTEF Proceedings
SINTEF Proceedings is a serial publication for peer-reviewed conference proceedings on a variety of scientific topics.
The processes of peer-reviewing of papers published in SINTEF Proceedings are administered by the conference organizers and proceedings editors. Detailed procedures will vary according to custom and practice in each scientific community.

PREFACE

This book contains all manuscripts approved by the reviewers and the organizing committee of the 12th International Conference on Computational Fluid Dynamics in the Oil & Gas, Metallurgical and Process Industries. The conference was hosted by SINTEF in Trondheim in May/June 2017 and is also known as CFD2017 for short. The conference series was initiated by CSIRO and Phil Schwarz in 1997. So far the conference has been alternating between CSIRO in Melbourne and SINTEF in Trondheim. The conferences focuses on the application of CFD in the oil and gas industries, metal production, mineral processing, power generation, chemicals and other process industries. In addition pragmatic modelling concepts and bio-mechanical applications have become an important part of the conference. The papers in this book demonstrate the current progress in applied CFD.

The conference papers undergo a review process involving two experts. Only papers accepted by the reviewers are included in the proceedings. 108 contributions were presented at the conference together with six keynote presentations. A majority of these contributions are presented by their manuscript in this collection (a few were granted to present without an accompanying manuscript).

The organizing committee would like to thank everyone who has helped with review of manuscripts, all those who helped to promote the conference and all authors who have submitted scientific contributions. We are also grateful for the support from the conference sponsors: ANSYS, SFI Metal Production and NanoSim.

Stein Tore Johansen & Jan Erik Olsen

Organizing committee:

Conference chairman: Prof. Stein Tore Johansen
Conference coordinator: Dr. Jan Erik Olsen
Dr. Bernhard Müller
Dr.Sigrid Karstad Dahl
Dr.Shahriar Amini
Dr.Ernst Meese
Dr.Josip Zoric
Dr.Jannike Solsvik
Dr.Peter Witt

Scientific committee:

Stein Tore Johansen, SINTEF/NTNU
Bernhard Müller, NTNU
Phil Schwarz, CSIRO
Akio Tomiyama, Kobe University
Hans Kuipers, Eindhoven University of Technology
Jinghai Li, Chinese Academy of Science
Markus Braun, Ansys
Simon Lo, CD-adapco
Patrick Segers, Universiteit Gent
Jiyuan Tu, RMIT
Jos Derksen, University of Aberdeen
Dmitry Eskin, Schlumberger-Doll Research
Pär Jönsson, KTH
Stefan Pirker, Johannes Kepler University
Josip Zoric, SINTEF

CONTENTS

MODELLING AND MEASUREMENTS IN THE ALUMINIUM INDUSTRY - WHERE ARE THE OBSTACLES?

Eirik MANGER[1]

[1] Hydro Aluminium, PMT, Hydrovegen 67, Porsgrunn, NORWAY

* E-mail: eirik.manger@hydro.com

ABSTRACT

In this paper the necessity of obtaining experimental data with good enough quality for model verification is addressed. Relevant examples from the aluminium industry are shown to illustrate some cases where measurements and model results work hand in hand on identifying bottlenecks and improving the situation. Moreover, measurements and their interpretation are briefly touched upon, trying to enlighten a few of the challenges on data collection in industrial environments and comparison with models.

Realising that measurements only uncovers parts of the real picture, an approach to estimate data interpretation errors is briefly outlined. A good model can and should rule out erroneous measurements – with the right use it can even give some guidelines on where to get good measurements.

Keywords: Measurements, CFD, Aluminium, Ducting.

NOMENCLATURE

Greek Symbols

ρ Mass density, [kg/m^3].

Latin Symbols

C Constant, [-].
p Pressure, [Pa].
u Velocity, [m/s].

INTRODUCTION

The development in computer hardware combined with more sophisticated modelling tools have during the last decades opened up a wealth of new possibilities to understand and explain physical phenomena in complex systems. This is indeed true also for the aluminium industry, where the processes range from "simple" gas flow all the way to multiphase flow and phase changes coupled with electromagnetic forces.

Models are however still only approximations of the real processes, and comparison with measurements is crucial and necessary. A previous presentation Manger (2014) showed the importance of correct problem descriptions. Along the same line, and equally important, are the access to and the quality of experimental data.

In this paper modelling combined with measurements are used to identify bottlenecks and other challenges in gas flow duct systems. Two different case studies will be used as examples, focusing on the area between matches and differences.

CASE STUDY I

The first case study is concentrated around a suction system for a quite old pot line, built in the mid 80's. Significant pressure drop increase in the ducting system during the last years has reduced the net pot suction rates and led to an unacceptable situation in terms of plant emissions. Measurements pointed towards deposits in the system, but there were questions on where and how much.

Original ducting system

Before moving on to the problem analysis, a brief overview of gas suction systems and their designs in aluminium plants is given.

Design

Gas suction systems for aluminium plants start at the individual pot by collecting fume gases from underneath the hooding. This is done via a gas channel with distributed openings along the pot's length, usually located behind the anode beams at the top of the superstructure – see Figure 1. To avoid emissions from the pot, the suction rates must be high enough to keep the fume gases inside the pot hooding. Necessary rates will depend on i.a. hooding efficiency, size and temperature, typically varying from 4500 to 6500 Nm^3/h/pot. Insufficient suction rates on the pots will cause undesirable emissions to the pot room and to the environment.

Figure 1: Gas channels at the top of the super structure.

Designing pot gas channels is a relatively straight-forward task, with a few guidelines:

- Pressure drop should be quite low
- Deposits in the channel should be avoided
- The suction should be even along the entire pot
- The construction must be simple and robust

Avoiding deposits in the pot gas channels can be (and often is) a challenge, particularly at the opposite end of the outlet where the channel dimensions lead to low velocities. This again changes the properties of the system and has undesirable effects.

The suction rate from each individual pot is controlled by dampers. The fume gas is led into one of several larger branches transporting the gas towards the Fume Treatment Plant, shortened FTP. Number of pots per branch varies, typically from 16 to 32, but there are systems with as many as 60 pots on one single line. Figure 2 shows the particular gas systems of interest, including which pot numbers that are connected to the different sections. The system might not look impressive at first glimpse, but the reader should note that the total length of the channels is 500 metres, with channel cross sections varying from 2.5 m^2 to approximately 8 m^2. The main inlets to the FTP have a cross section of nearly 30 m^2.

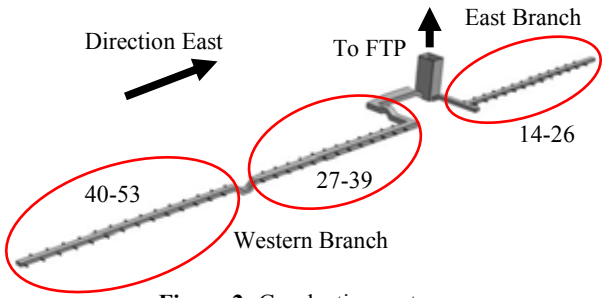

Figure 2: Gas ducting system.

Modelling

To get an impression of the ducting system performance, several CFD models were established.

First the sizes of the opening slots in the pot gas channel were investigated. A simple model based the existing layout was established having ~24K hexahedral cells. Constant density for air at 120°C was assumed, and the Relizable k-ε model handled turbulence. The flow distribution could then be determined by using a pressure inlet with a fixed outlet flux. Slot sizes decrease towards the outlet to compensate for the increased suction pressure (lower static pressure), mainly caused by increased gas velocity towards this side. The geometric model is shown in Figure 3, whereas the predicted static pressure just outside and inside the pot gas channel is shown in Figure 4.

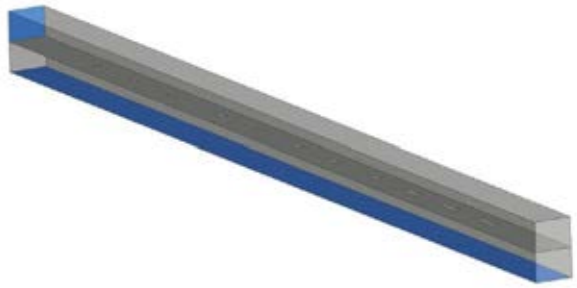

Figure 3: Geometric model, pot gas channel.

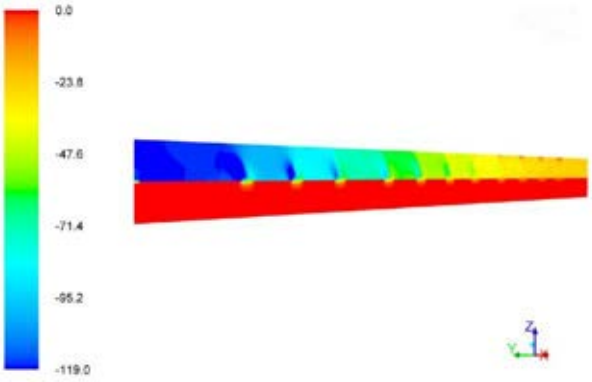

Figure 4: Static pressure outside and inside the pot gas channel.

Analysing the flux through each of the slots revealed that the openings towards the outlet actually were too small, as can be seen in Figure 5. By adjusting the size of these, a more even suction from the pot could be achieved. In addition, the net pressure drop through this part of the system was reduced with nearly 25%.

The CFD model for the entire duct system became a bit more complicated. A mesh with approximately 3.8M polyhedral cells was constructed. Similar models and boundary conditions as for the hooding simulations were used, except that the inlet pressure from each pot had to be handled separately.

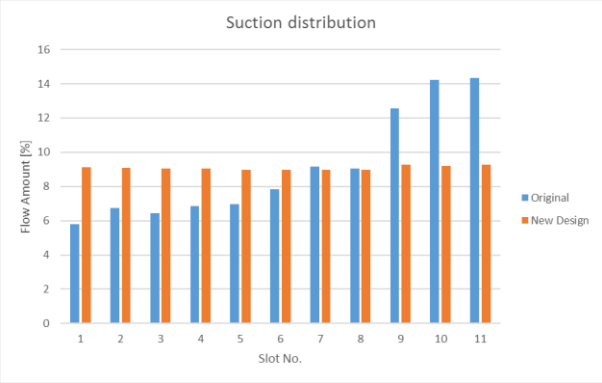

Figure 5: Original and new suction distribution.

Adding the measured pressure drop through the interface towards the ducting branches (will be touched upon later) gave a reasonable estimate for the total inlet pressure drop into the channel. This pressure drop is modelled as a turbulent dynamic resistance on the form

$$\Delta p \approx C \cdot \frac{1}{2} \rho u^2 \qquad (1)$$

The calculated pot suction rates for the unbalanced system are depicted in Figure 6. The results show, as expected, that the pots closest to the FTP intake have significantly higher suction rates compared against the end pots. Furthermore, the branch east of the FTP inlet generally have more suction compared to the western branch. This is also as expected, since there are a number of restrictions along the western flow path.

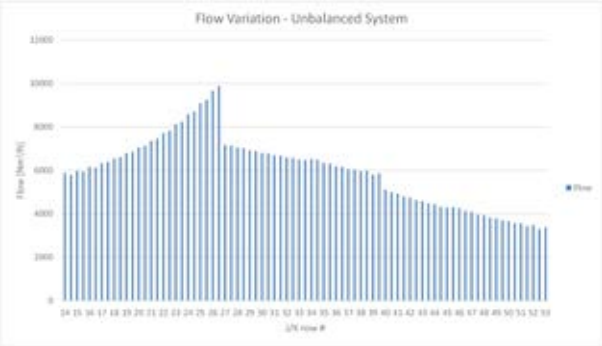

Figure 6: Calculated flow rates for an unbalanced system.

Before moving on to investigate if, and if so where, there are deposits in the system, the flow must be balanced theoretically. In real life this is done by measurements, so there might be some deviations to the actual damper settings, but this represents the closest match achievable between modelling and measurements.

The estimated resistance coefficients for balancing the system are shown in Figure 7. From correlations it can be shown that a resistance factor of around 4 represents blocking approximately half the available flow area. After balancing the systems, the average flow rate is predicted to some 6000 Nm^3/h/pot at 130°C and a suction pressure around 1500 Pa at the FTP inlets.

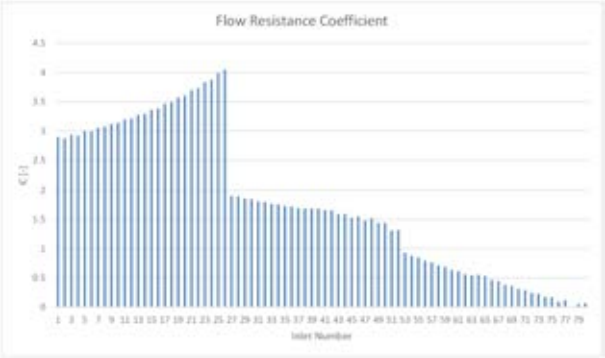

Figure 7: Estimated resistance coefficients for balancing the suction system.

Deposit analysis

With a balanced system in place, the search for obstacles and deposits could commence. Measured static pressures are shown in Figure 8. These correspond to effective suction pressures on the pots and were obtained by M. Karlsen (2016). Pots 1 to 13 in the series are connected to another FTP and not subject to analysis here, so focus should be on the pots in the range from 14 to 55. A first inspection shows that there is a big jump in suction pressure between the pots 40 and 41.

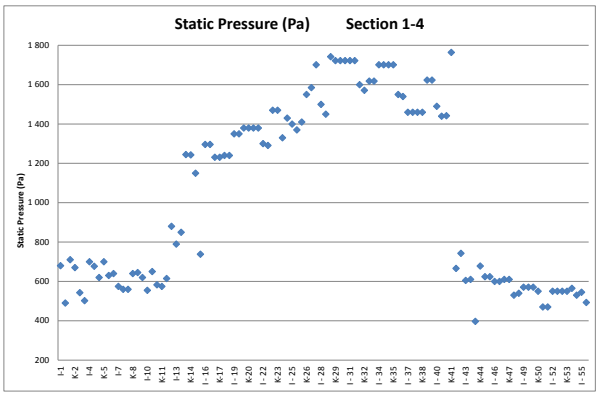

Figure 8: Measured suction pressure in the system.

Putting the simulation results on top of this shows that there is also a predicted jump in the pressure profile not seen in the measurements. In addition to the rather obvious restriction between pots 41 and 42, this indicates that something might be blocking the path from the eastern branch as well.

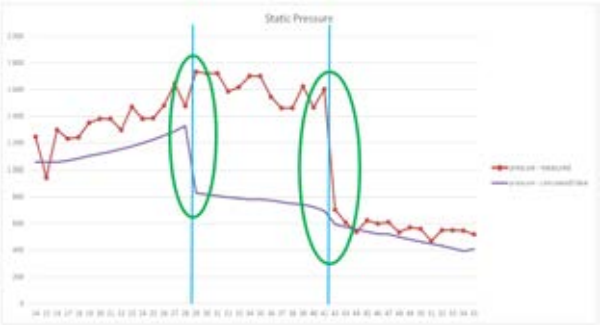

Figure 9: Comparison between simulated and measured pressure profile.

To investigate the effect of deposits and put numbers on the amount of material, the geometry was altered by blocking part of the lowest section in the channel dip, as can be seen in Figure 10. By trial error the deposit height in the channel dip was predicted to around one meter, leaving an open space only around 60 cm high from the originally 165 cm. Again, the pictures might not justify the dimensions – with one meter deposits as shown here, the blocked volume is some 12-13 m^3.

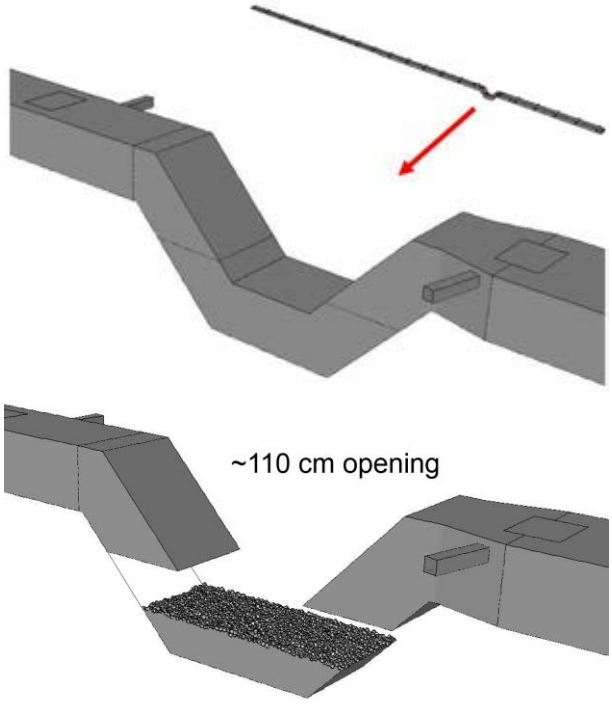

Figure 10: Top; the original channel dip layout. Bottom; channel dip partially filled with deposits.

The yellow line in Figure 11 shows the revised pressure profile with deposits in the channel dip. The match between measurements and simulations is now quite good for the eastern part of the system. By adding a restriction between the FTP inlets and the western branch, an even better agreement can be achieved, as shown with the green line. The amount of deposits and exact location for this have however not been followed further in the simulations.

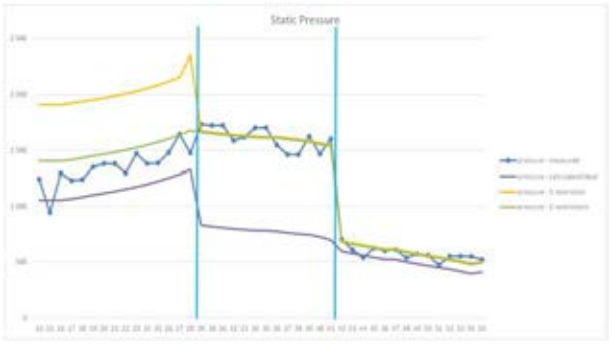

Figure 11: Estimated resistance coefficients for balancing the suction system.

Optimising the pot gas channel

In a situation where every extra Pascal of suction pressure matters in trying to improve the emissions, especially for the end pots, also the construction of the pot channel interface towards the gas channel branch has been addressed. The original design had several obstructions and small openings, which can be seen in Figure 12. Streamlining, removing obstacles, and increasing the smallest openings with minor adjustments, as showed in Figure 13, reduce the pressure drop with approximately 25%, which also will contribute to larger net suction rates for the pots.

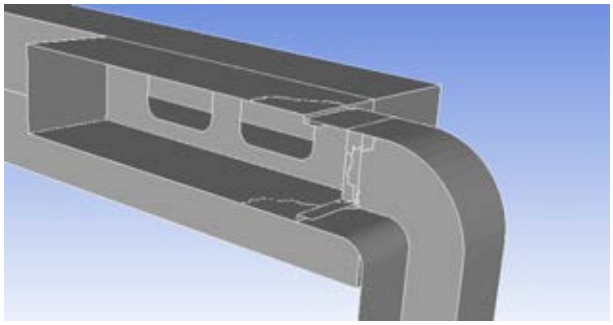

Figure 12: Original pot channel outlet.

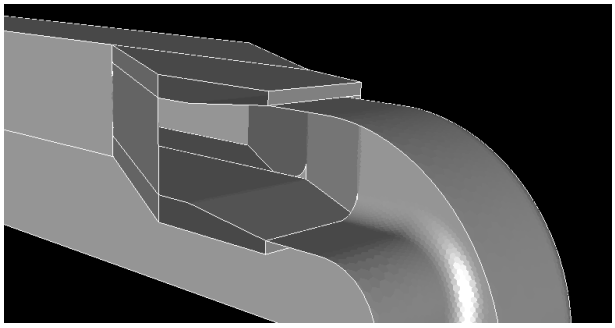

Figure 13: Optimised pot channel outlet.

Current status

Comparing measurements and calculations strongly indicated that deposits reduced the pot suction rates significantly upstream the channel dip in the western branch. Opening some small hatches confirmed these conclusions, and actions could be planned.

Deposit removal

With evidence on significant amounts of deposits in the channel dip, it was decided to send in personnel to inspect the situation. Large amounts of rock solid material were found at the bottom, and the smallest opening height was measured to around 60 cm – in very good agreement with the simulations. It was further decided to try to remove some of the deposits.

Before starting the work, however, a there was a question asking how much of the material that should be removed to see an impact on the end pots. Thus, a series of simulations were run looking at the dependence between end pot suction rate and deposit height. Results from the simulations, plotted in Figure 14, show that there seems to be a minimum threshold value around

one meter. For opening heights larger than this, the net gain of removing deposits is relatively low per unit, whereas below this value the suction pressure on the end pots decrease rapidly.

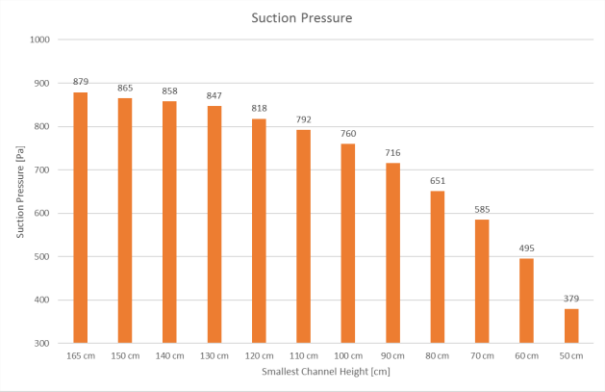

Figure 14: Effect of smallest opening height on end pot suction rate.

Personnel has done a magnificent job in digging and removing deposited material from the channel dip. Currently the smallest opening height has been increased to almost one meter, as recommended from the calculations. The duct system has responded well, again in quite good agreement with the model, and the suction pressure on the end pots is now close to 800 Pa.

Superstructure modifications

The proposed changes on the pot gas channel interface has also been accepted by the plant management. The changes are implemented when the pots are relined, and will slowly contribute to an even better emission picture.

Final comments

This work has shown how measurements combined with CFD models can be used to analyse and identify obstacles in a gas ducting system. The essence, perhaps not stated very directly, is that even quite simple models (no boundary layers, k-ε based turbulence model etc.) perform well enough when uncertainties on e.g. geometry, deposits and measurements are added to the picture. There is no point in striving for the last 1% accuracy in simulation models when other deviations easily can be a factor 10-20 above this. For us this is pragmatic modelling.

CASE STUDY II

The second case study is also concentrated around a suction system for a rather old pot line. Increasing the line current has altered the performance, and larger suction rates were needed to avoid substantial emissions.

Rather than looking at the entire system, the focus will be towards the suction rates from single pots. When analysing the system, there were large discrepancies between pitot tube measurements and the simulation results. To explain these differences a deep dive into measurement interpretation was needed, forming a basis of what could be referred to as model assisted measurements.

Superstructure gas channel

To get an understanding of the pots' suction rates, the superstructure gas channels were simulated. Again a very simple model with some 54K polyhedral cells, constant density, Relizable k-ε, in combination with pressure inlet and fixed mass outflow, but it should still be able to capture the main features of the design. The geometric layout is shown in Figure 15, whereas the predicted velocities are plotted below in Figure 16. The velocities at the inlets are quite low, and the channel outlet velocity is around 16 m/s.

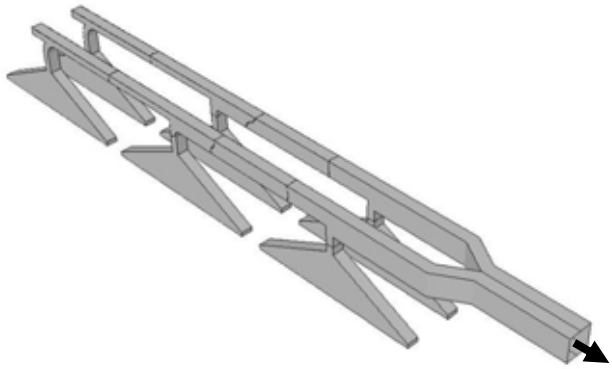

Figure 15: Gas channel design in the superstructure.

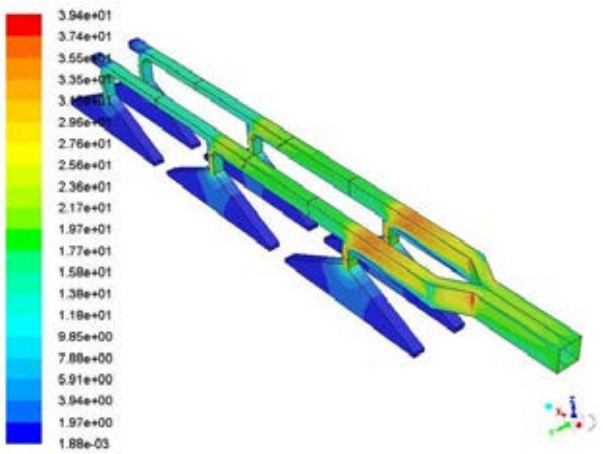

Figure 16: Predicted velocities in the superstructure gas channel.

In general, the pressure drop through the superstructure gas channel will depend on the flow rate as well the density – or implicitly, on temperature. Figure 17 shows the relationship between pressure drop and flow rate, given in units of Nm^3/h (which actually is equivalent to a mass flow rate), for three different temperatures.

In addition, the pressure drop is given for two different states of the gas channel. The inlets from each hooding contain dampers to control and balance the flow. When fully open, the gas suction is not even along the pots. When balancing the flow, the pressure drop is increased with some 30%.

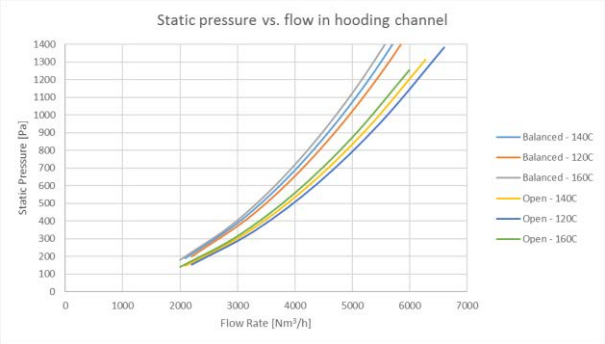

Figure 17: Gas channel design in the superstructure.

Ideally, calculated flow rates should of course match the measurements. However, when comparing these, there were large deviations, as can be seen in Figure 18. Here only the pressure drop curves for 140°C have been shown for simplicity. The estimated flow rates, from seven profile points across the pipe using a pitot tube, seem to indicate pressure drops of the order 800 Pa for flow rates around 6000 Nm^3/h. The calculations predict 1100-1200 Pa at the same rates – or even higher if the superstructure gas channel was balanced.

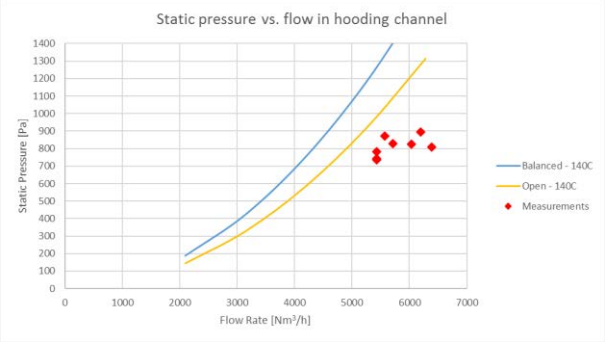

Figure 18: Comparing measurements with simulation results.

Measurement interpretation

In search for explanations there were no reasons to disbelieve in the measurements – these were of excellent quality, with low variation and good repeatability. At the same time, adjusting and refining the CFD model had little impact on the calculated pressure drop.

After some discussions back and forth, the measurement interpretation came up as a point that might be questioned. Due to the channel outlet design, which has an expander from Ø200 to Ø460, and the location of the measurement point just downstream of this (access restrictions), the measured velocities showed a clear parabolic profile in the pipe, see Figure 19. Since the flow is highly turbulent, such a profile is not exactly expected, also indicating that the flow is not fully developed. In addition, for a circular pipe as measured here, the cross-sectional area covered by each point increases radially. Thus, utilizing our standard way of measurement interpretation, i.e. simple averaging, might not be good enough in this case.

The reader should note that the number of points in the velocity profile plot differs from the actual number of measurements points. Using an interpretation template, the user should specify both wall distance from first/last point, as well as the distances between the points. The values at the wall, constituting the first and the last points in the velocity profile, can either be set to zero or be found from extrapolation – representing a best possible reconstruction of the velocity profile.

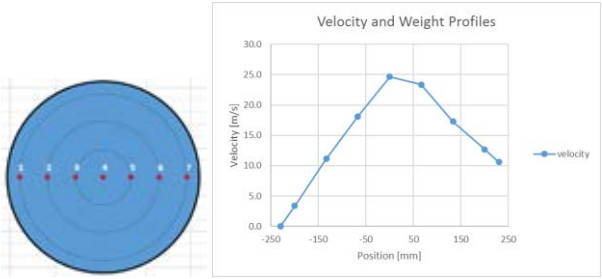

Figure 19: Measured velocity profile and corresponding measurement points.

To overcome the hurdles on measurements/model discrepancy, a revised method on measurement interpretation was outlined and used. The method will be discussed briefly in the next section, but for now concentrate on the numbers found. The new interpretation puts the pressure drops as function of flow rates right on top of the model predictions, see Figure 20, and it was concluded that this was the main cause for the deviations.

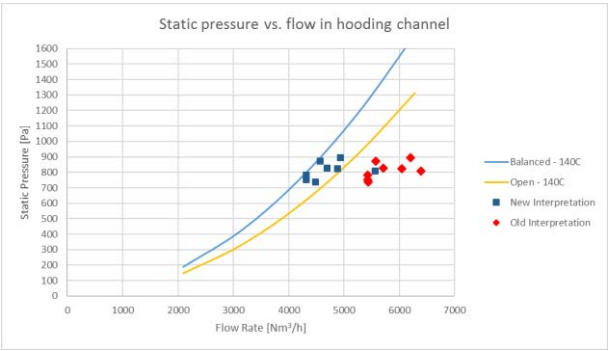

Figure 20: Changing the measurement interpretation.

Model assisted measurements

It is no understatement to claim that out in the field, measurements must often be performed based on availability, which not necessarily corresponds to the optimal location. Based on the findings in this last project, there is now a recommendation on always combining measurements and models with the aim to say something about the conditions at the measurement location.

To give an example of how interpretation can influence the flow predictions from measurements, two rather simple geometries are considered – a straight pipe and an expander, the last one being showed in Figure 21.

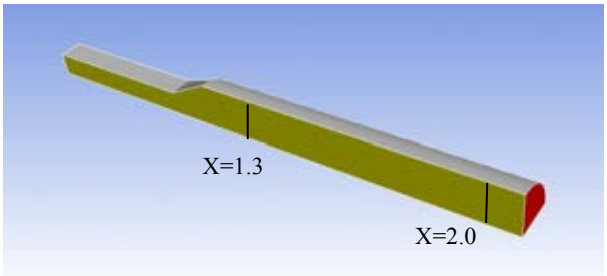

Figure 21: The expander, to be measured virtually.

The flow is simulated using a fixed velocity inlet, and monitoring points are added at two downstream locations to measure velocities virtually. These are then again used to calculate the flow rates (or rather the mean velocity). Three different approaches for calculating the mean velocity are considered:

- Simple arithmetic averaging
- Area weighted averaging
- Linear reconstruction of the velocity profile

The results from the virtual measurements are given in Table 1, whereas the calculated mean velocities and the deviations when using the different methods are shown in Table 2. Note that the real average velocity should be around 8.9 m/s.

As can be seen from the tables, there are only small discrepancies for the straight pipe section, independent of which calculation method used. For the expander, the story is however quite different. Close to the expander (at X=1.3), the mean velocity based on arithmetic averaging is overestimated with 50%. Using area based averages improves the figure somewhat, but there is still a deviation of almost 35%. The calculation based on linear reconstruction of the velocity profile is however superior to the others, with only 10% deviation even at this position (which is quite close to the expansion and far from optimal). Further downstream the expansion the deviations decrease.

Table 1: Virtual measurements in a pipe and an expansion.

	Straight		Expansion	
Point No.	*X = 1.3*	*X = 2.0*	*X = 1.3*	*X = 2.0*
1	8.96	9.13	8.7	8.8
2	8.97	9.23	14.5	9.7
3	8.97	9.23	15.3	10.3
4	8.97	9.23	15.3	12.5
5	8.97	9.23	15.3	10.3
6	8.97	9.23	14.5	9.7
7	8.96	9.13	8.7	8.8

Table 2: Estimated mean velocities based on the virtual measurements, and the deviations from real values.

	Straight		Expansion	
Method/Variable	*X = 1.3*	*X = 2.0*	*X = 1.3*	*X = 2.0*
Avg. Velocity				
Simple Aritmetic	9.0 m/s	9.2 m/s	13.2 m/s	10.0 m/s
Area Weighted	9.0 m/s	9.2 m/s	11.8 m/s	9.4 m/s
Linear Flow Interp.	9.0 m/s	9.1 m/s	9.8 m/s	9.1 m/s
Deviation				
Simple Aritmetic	1.9 %	4.6 %	49.8 %	13.8 %
Area Weighted	1.9 %	4.3 %	34.2 %	7.0 %
Linear Flow Interp.	1.8 %	3.9 %	11.2 %	3.2 %

The latter represents an example on how to use simulations in "assisting" with interpretation and perform quality control of measurements. In the future more work will follow this line.

CONCLUSION

The conclusions are:

1. With the powerful CFD tools available today, simulation errors due to e.g. model selection or settings are often smaller than the measurement errors in an industrial environment. This is of course true only if the models are utilized in a correct manner.
2. Measurements, even though not of the best quality, can hand in hand with simulations prove to be a valuable tool for finding faults and obstacles in existing systems. Keep focus on the discrepancies.
3. Always have a knowledge of what is measured and how to interpret and convert the results into other numbers. A wrong interpretation and understanding will evidently lead to inaccurate figures and deviations.

ACKNOWLEDGEMENT

Interaction between measurements and modelling is a teamwork requiring expertise in both areas. The author wishes to acknowledge M. Karlsen and A. Dyrøy (2016) for excellent field work, discussions and contributions through the work.

REFERENCES

MANGER, E. (2014), "CFD in Problem Analysis and Optimisation – the Importance of Correct Boundary Conditions", *Proc. CFD 2014 – 10th Int. Conf. on CFD in the Oil & Gas, Metallurgical and Process Industries,* Trondheim, Norway, June 17-19.

KARLSEN, M. and DYRØY, A. (2016), *Private Communications.*